Surface Minimal Bactericidal Concentration: A comparative study of active glasses functionalized with different-sized silver nanoparticles

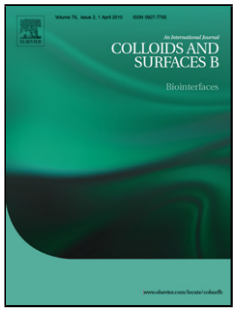

Surface Minimal Bactericidal Concentration: A comparative study of active glasses functionalized with different-sized silver nanoparticles

Giulia Barzan (Methodology) (Investigation) (Data curation) (Writing - original draft) (Writing - review and editing), Luca Rocchetti (Methodology) (Investigation) (Data curation), Chiara Portesi (Methodology) (Data curation), Francesco Pellegrino (Methodology) (Investigation) (Data curation), Angelo Taglietti (Conceptualization) (Writing - review and editing), Andrea Mario Rossi (Funding acquisition) (Supervision) (Writing - review and editing), Andrea Mario Giovannozzi (Conceptualization) (Resources) (Data curation) (Writing - review and editing) (Supervision)

PII: S0927-7765(21)00244-7

DOI: https://doi.org/10.1016/j.colsurfb.2021.111800

Reference: COLSUB 111800

To appear in: *Colloids and Surfaces B: Biointerfaces*

Received Date: 19 January 2021

Revised Date: 20 April 2021

Accepted Date: 26 April 2021

Please cite this article as: Barzan G, Rocchetti L, Portesi C, Pellegrino F, Taglietti A, Rossi AM, Giovannozzi AM, Surface Minimal Bactericidal Concentration: A comparative study of active glasses functionalized with different-sized silver nanoparticles, *Colloids and Surfaces B: Biointerfaces* (2021), doi: https://doi.org/10.1016/j.colsurfb.2021.111800

Surface Minimal Bactericidal Concentration: A comparative study of active glasses functionalized with different-sized silver nanoparticles

Giulia Barzan[a,b], Luca Rocchetti[c], Chiara Portesi[a], Francesco Pellegrino[c], Angelo Taglietti[d], Andrea Mario Rossi[a] and Andrea Mario Giovannozzi[a*]

[a] *Quantum Metrology and Nano Technologies Division, Istituto Nazionale di Ricerca Metrologica (INRiM), Strada delle Cacce, 91, 10135 Turin, Italy;*

[b] *Departement of Electronics and Telecommunications, Politecnico di Torino, Corso Duca degli Abruzzi, 24, 10129 Turin, Italy;*

[c] *Department of Chemistry and NIS Inter-Departmental Centre, University of Torino, Via Pietro Giuria, 9, 10125 Turin, Italy*

[d] *Department of Chemistry, General Chemistry Section, University of Pavia, viale Taramelli, 12, 27100 Pavia, Italy;*

[*] *Corresponding author: Andrea Mario Giovannozzi, tel +39 011 3919330; e-mail a.giovannozzi@inrim.it*

Graphical abstract

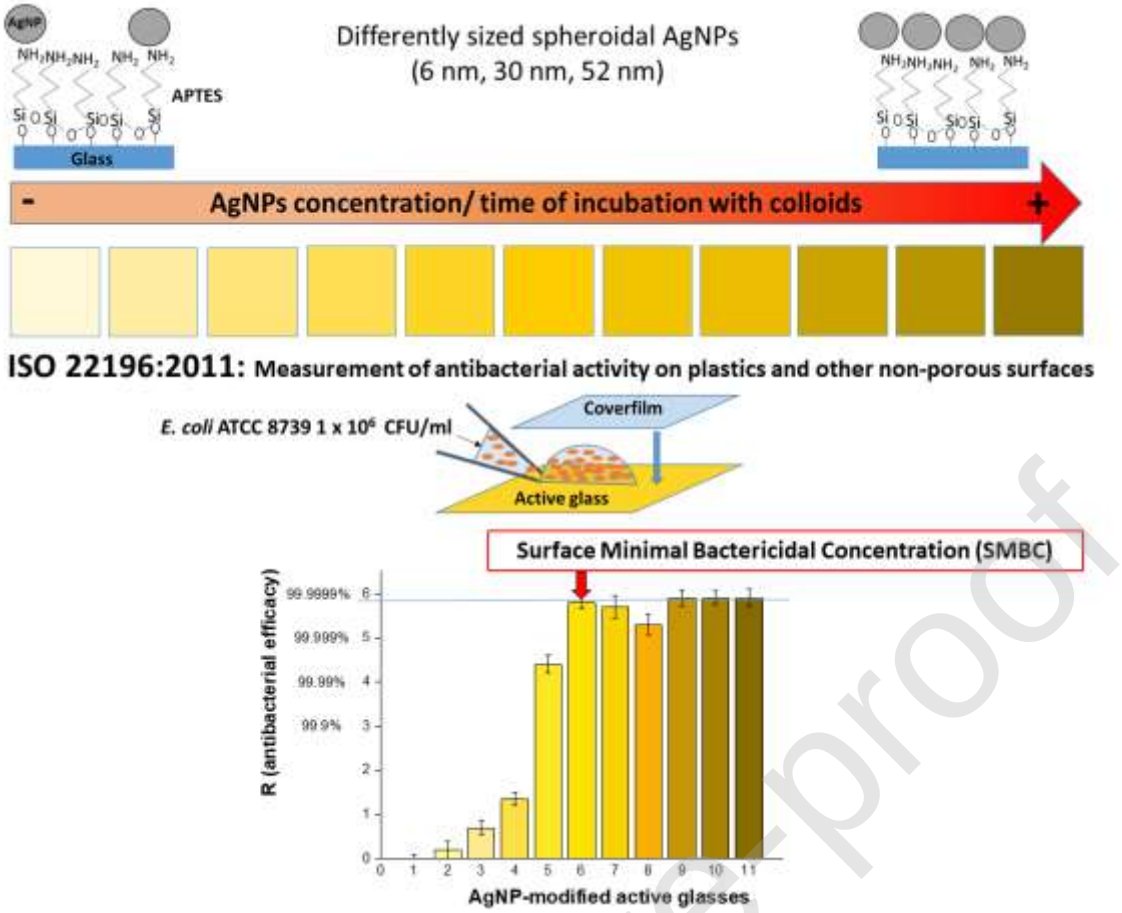

Highlights

- Differently sized spheroidal AgNPs are prepared and tested against *E. coli*
- AgNPs are immobilized on amino-silanized glasses with different surface coverage
- Antibacterial efficacy of active glasses is tested by ISO 22196 against *E. coli*
- Surface Minimal Bactericidal Concentration (SMBC) is found for each AgNPs size
- SMBC is applied to reach the maximum bactericidal effect with the minimum of silver.

Abstract

In this work the quantification of antimicrobial properties of differently sized AgNPs immobilized on a surface was studied.. Three different sizes of spheroidal AgNPs with a diameter of (6, 30 and 52) nm were synthetized and characterized with UV-VIS, SEM, TEM and ICP-MS. The MIC (Minimal Inhibitory Concentration) and MBC (Minimal Bactericidal Concentration) against *Escherichia coli* were investigated. Then, the antibacterial efficacy (R) of amino-silanized glasses coated with different amounts of the three sizes of AgNPs were quantified by international standard ISO 22196 adapted protocol against *E. coli*, clarifying the relationship between size and antibacterial properties of immobilized AgNPs on a surface. The total amount of silver present on glasses with an R ~ 6 for each AgNPs size was quantified with ICP-MS and this was considered the Surface MBC (SMBC), which were found to be (0.023, 0.026 and 0.034) μg/cm^2 for (6, 30 and 52) nm AgNPs, respectively. Thus, this study demonstrate that active surfaces with a bactericidal effect at least ≥ 99.9999 % could be obtained using an amount of silver almost 100 times lower than the MBC found for colloidal AgNPs. The immobilization reduces the aggregation phenomena that occur in nanoparticles promoting direct contact with bacteria. Starting from this glass model system, our work could broaden the way to the development of a wide range of antibacterial materials with very low amount of silver that can be safely applied in biomedical and food packaging fields.

keywords: silver nanoparticles, E. coli, antibacterial properties, surface minimum bactericidal concentration, glass silanization, APTES

1. Introduction

Recently, silver nanoparticles (AgNPs) have risen great interest in many fields due to their low tendencies to develop microbial resistance [1], broad spectrum killing [2] and unique plasmonic properties in the visible region [3]. Colloidal silver has already demonstrated its bactericidal and antiviral effect [4] that can be explained by damage to the cell membrane and intracellular metabolic activity [5]. However, silver in low concentrations, as 0.01 mg/m^3, is not toxic for human and animal cells [6] and is considered environmentally friendly, even if some concern is raised for the overall impact on health and environment. As a result, AgNPs have emerged as the most widely used nano-antimicrobial in many consumer products, food packaging [7], medical implants [8] and water disinfection applications[9]. Size is normally considered a key factor in the antibacterial activity of AgNPs, indeed several studies [10–12] observed a gradual increase of such activity as size decreases from 100 nm to 20 nm, with a dramatic enhancement as the size gets down at the sub-10 nm scale. Higher microbicidal effect can be expected from smaller particles because they have a higher exposed metallic surface [13] and a faster ion release [14]. In addition, the shape was found to affect antibacterial activity of AgNPs. Results from Pal et al. [15] demonstrated that truncated triangular nanosilver exhibited the highest biocidal activity followed by silver nanospheres and nanorods. Since most of these antibacterial studies were conducted in liquid, many results such as those from Kvítek et al. [16] and Radniecki et al. [17], demonstrated how the dispersion and chemical stability influence antibacterial activity of AgNPs with a significant decrease of the MIC when a surface modifier is used. However, very little is known on the relations between size and bactericidal properties of immobilized AgNPs [18]. Several studies

demonstrated the antibacterial properties of different types of surfaces, such as bio/polymers [8,19], fabrics, textiles [20] or glass [21], coated or incorporated with AgNPs. However, to the authors' knowledge, a comparative study on the size effect and on the surface loading of the AgNPs in respect to the antibacterial properties is not present. In this work, three different sized AgNPs (6 ± 3, 30 ± 6, 52 ± 7) nm were produced and characterized for shape, dimensions, dispersion in liquid medium and Ag content. MIC and MBC against the Gram negative bacterium *Escherichia coli* were investigated in liquid to confirm the highest bactericidal effect of the smaller AgNPs. Then, monolayers of all the three sizes of AgNPs were obtained on a model glass surface using the ''layer-by-layer" (LbL) approach described by Taglietti et al. [21]. Glass slides with different percentage of coverage were prepared and their antibacterial property against *E. coli* was quantified by the international standard ISO 22196 to evaluate i) the dependence of the bactericidal effect on the AgNPs size and ii) to quantify the Surface MBC (SMBC) for each type of AgNPs modified surface. Moreover, a comparison analysis on the MBC and the SMBC is discussed to better elucidate the different mechanisms of action and the overall antibacterial performance in these two different configurations.

2. Material and Methods

2.1 Chemicals

Silver nitrate (>99.8%), sodium borohydride (>99.0%), sodium citrate (>99.0%), (3-mercaptopropyl)trimethoxysilane (≥98%, APTES), Luria Barthani (LB) broth, LB agar, PBS tablets pH 7.4 (for 200 ml) and Nutrient broth (NB) components were purchased by Sigma

Aldrich and diluted in Milli-Q water.

Plate count agar (PCA), Soybean casein digest broth and polyoxyethylene sorbitan monooleate (SCDLP), Phosphate-buffered physiological saline (PPS) were prepared in Milli-Q water. All the solutions used for the bacterial analysis were autoclaved.

2.2. Colloidal Nanoparticles preparation

The synthesis of spheroidal silver nanoparticles was adapted from a previously reported preparation [22–24]. Briefly, silver nitrate was reduced by sodium borohydride under controlled conditions of temperature to produce seeds with a diameter of about 6 nm which were used as initiators to the subsequent growth of larger nanoparticles based on the stepwise seeded-growth method.

2.3 Characterization of colloidal AgNPs

Absorbance spectra of colloidal AgNPs were taken with a UV-VIS spectrophotometer (Lange DR500) in the 200-1000 nm range. Milli-Q water was used as blank.

Transmission electron microscopy (TEM) images were collected with a Jeol JEM-3010 UHR instrument with a point resolution of 0.17 nm, equipped with monocrystalline LaB_6 as thermo-ionic source, using a voltage of 300 kV. A drop of colloidal suspension of AgNPs, prepared as described, was deposited on a copper grid (3 mm) covered with a perforated carbon thin film and left to air dry before the analysis. TEM images were processed with ImageJ software [25] to calculate the relative diameter and the function of distribution of the dimensions of the colloids. For this purpose, at least 200 NPs were analyzed by TEM micrographs for each AgNPs size.

Thermo Fisher Scientific ICP-MS ICAP-Qs model was used to quantify the Ag concentration in each AgNPs preparation. The samples were previously sonicated for 20 min at 80W, filtered with a 0.2 µm Nylon filter and washed three times with Milli-Q water by centrifugation (details in SI). Then, 0.5 ml of the suspensions were mineralized in hot concentrated HNO_3 to guarantee a complete silver solubilization and diluted up to 1: 10˙000 with a final nitric acid concentration of 2% v / v.

The calibration curve was constructed with 7 points (100, 50, 25, 10, 5, 1 and 0.3) µg/l and linear correlation coefficient > 0.999. Interference due to polyatomic ions is eliminated by operating the collision cell in He mode with kinetic energy discrimination (He - KED). ^{107}Ag was used for quantitation. Other parameters as follows: RF power 1450 W; Main Ar Flow 15 l/min; Ar auxiliary flow 1.0 l/min; Nebulizer flow 0.90 l/min; Concentric nebulizer with impact sphere; Collision cell He flow 5.0 ml/min. Extraction Lens voltages and KED bias auto-optimized with the tuning solution suggested by the vendor.

2.4 Bacterial strain and culture conditions

E. coli ATCC 8739 strain was used for the microbiological experiments. The culture conditions for the MIC and MBC experiments for both colloidal AgNPs and AgNPs-modified glasses are explained in details in SI.

2.5 Solid surfaces functionalization

Microscopy glass slides (26 x 76 mm, 1.0-1.2 mm thick) were cut manually in squares of 25 mm x 25 mm, cleaned firstly in Acetone and Ethanol, then with aqua regia (3:1 HCl 37% : HNO_3 65%) for 15 min, washed three times with ultrapure water, immersed in piranha solution (3:1 H_2SO_4 96% : H_2O_2 30%) for 30 min at 80° C and washed other three times with

ultrapure water. Glasses were then soaked for 1 hour in a 3% (v/v) solution of (3-aminopropyl)triethoxysilane in methanol at room temperature. 4 glass slides were prepared at the same time, i.e. reacting in the same APTES solution inside a teflon slides holder (positioned vertically). After this, the amino-modified glasses were washed under sonication with methanol, dried under a nitrogen stream, moved to a 4-place glass holder and kept thermostatically at 150°C for 1 hour. After cooling down to room temperature, they were incubated in 30 ml of colloidal AgNPs of the desired size and dilution for different times. The range of AgNPs concentrations used was between 1.9 μg/ml and 60 μg/ml while the tested incubations time vary from 15 min to O/N. The functionalized glasses were washed with ultrapure water and let air dry vertically.

2.6 Active glass characterization

Absorbance spectra of AgNPs-functionalized glass were taken with a UV-VIS spectrophotometer (Lange DR500) in the 200 nm -1000 nm range. Spectra were obtained placing the glasses in the apparatus equipped with a film holder, using a non-functionalized cleaned glass as blank.

Scanning electron microscopy (SEM) analysis of the glass slides was performed using a SEM FEI Inspect F in UHV. For preventing the charging of the samples, the samples were sputter coated with 10 nm of Au film. An acceleration potential of 10 kV, with a spot of 3.5 and a magnification of 10000X were used to acquire at least five images in different zones of the samples, to get the estimation of the average distribution of the nanoparticles on the glass surface. The images were analyzed with ImageJ and converted to binary to obtain the percentage of area covered by silver nanoparticles.

Quantification of Ag coverage on glass was performed on three selected glasses in duplicate, two for each AgNPs size. Glass slides without AgNPs, only functionalized with APTES, were analyzed as blank. AgNPs were detached from glasses by soaking the slides in HNO_3 65% for 3 hours and sonicated for 2 minutes, then the final volume was brought to 25 ml with HNO_3. The samples were then treated in microwave (30 min at 150°C) to dissolve the residual AgNPs and finally diluted to obtain a HNO_3 concentration of 5%. The solutions were then analyzed with the ICP-MS apparatus described in paragraph 2.3.

2.7 Antibacterial activities of AgNPs-modified glass slides

Performance testing of the glasses was principally conducted in accordance with ISO 22196:2011[26]. The ISO 22196:2011 stipulates the procedure for testing of antibacterial activity of plastics and states the ranges of test parameters. It determines the preparation of test specimens, culture conditions for test microbes, the incubation time, the content of nutrient medium, and the analytical method. However, the standards are not freely accessible and need to be bought. To avoid any legal repercussions we refer to the standard, all changes to the standard protocol are given in detail to clarify the experimental procedures. The glasses, both AgNPs-functionalized and untreated as controls, were sterilized in a 70% Ethanol bath for 20 min. The volume of the inoculum was reduced to 100 µl in proportion to the area of the sterile cover film, which in this case was reduced to 20 x 20 mm to maintain the correct dimensionality in relation to that of the glasses, in line with the ISO requirements. $1x10^6$ CFU/ml of bacteria were inoculated on each glass. The time of contact of *E. coli* with the surfaces was reduced to 5h to better appreciate the kinetics of the killing efficacy and to highlight main differences related to the AgNPs size and to their surface coverage.

3. Results and discussion

3.1 Characterization of different sized colloidal AgNPs

Three different sizes of citrate-capped spheroidal shaped AgNPs with a nominal diameter of 6 nm, 30 nm and 52 nm were produced by a *stepwise seeded growth* synthesis method, as described in paragraph 2.2 and characterized with different analytical techniques. Firstly, their shape and dimensions were determined with TEM (Fig.1 a)-b)-c)), while their optical properties and agglomeration state with UV-VIS spectroscopy (Fig.1 d)-e)-f)); then, a quantitative analysis on the total Ag in solution for every type of AgNPs was performed with ICP-MS. A summary of the physiochemical properties of the synthetized AgNPs, such as shape, size distribution, surface area and number of NPs, is reported in Table S1 (SI).

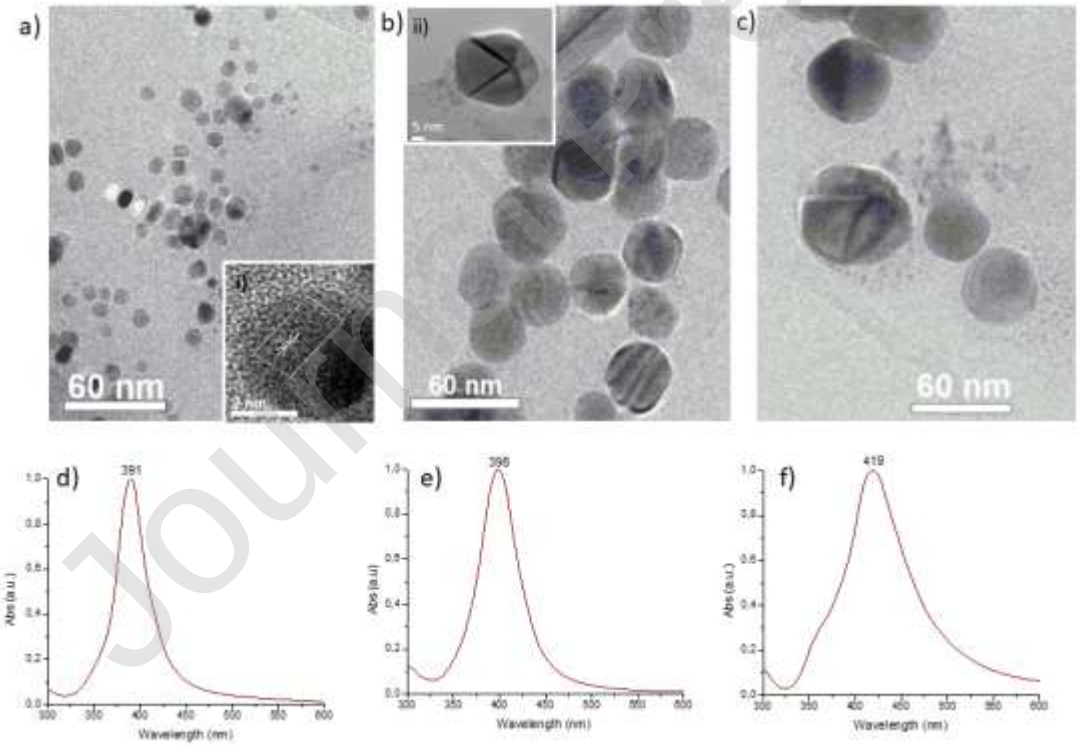

Fig.1 TEM and UV-VIS colloidal AgNPs characterization: a)-b)-c) TEM images of colloidal AgNPs 6 nm, 30 nm and 52 nm respectively. Inset i) High Resolution TEM image that shows the lattice fringes of a 6 nm nanoparticle. Inset ii) TEM image that shows a particular pyramidal shape of a 30 nm nanoparticle. **d)-e)-f)** UV-VIS absorbance spectra of colloidal AgNPs (6, 30, 52) nm from left to right respectively, with the reference maximum absorbance peaks.

TEM analysis revealed a spheroidal shape for all the synthesized AgNPs with the expected average diameters (Fig.1 a)-c)). TEM was also used to evaluate the crystallinity degree of the different samples. As the inset i) of Fig.1 shows, the distance between two crystallographic planes was measured as 2.4 Å for all the three samples, which is in accordance to data on single crystalline silver nanoparticles reported in literature [27], this *d-spacing* of lattice fringes corresponds to the (200) plane of silver. In case of AgNPs growth from seeds, i.e. AgNPs of 30 nm and 52 nm, HRTEM images showed the presence of multiple-twinned crystalline planes. In particular, the inset in Fig.1 b) ii) shows a five-fold multiple twinned decahedron crystal, which is favored for the growth of silver. The presence of multiple twinned particles normally indicates that silver nuclei/particles formed at the first stage undergo Ostwald ripening in the second stage and are transformed into larger silver nanoparticles, thus completing the growth process [12,28].

The UV-VIS extinction spectra can also provide information about the size, shape, size distribution and the agglomeration state of the synthetized AgNPs. As Fig.1 d)-e)-f) shows, the λ_{max} of the AgNPs UV-VIS spectra increases from 391 nm to 417 nm, showing a red-shift of the Local Surface Plasmon Resonance (LSPR) peak as the relative particle size increase from 6 nm to 52 nm [29]. Single, narrow and symmetric absorption peaks attests a good

homogeneity in terms of size distribution and spheroidal shape, which also was confirmed by TEM analysis.

The concentration of silver in each type of AgNPs stock was determined through ICP-MS analyses and the results are collected in Table S1 (SI).

3.2 MIC and MBC determination of colloidal AgNPs

MIC and MBC of the three differently sized colloidal AgNPs towards *E. coli* ATCC 8739 were investigated performing both broth dilution method (BDM) and CFU assay, as described by the National Committee for Control of Laboratory Standards (NCCLS) guidelines [30]. As Table 1 shows, the obtained MIC and MBC values are in good agreement with the already published data of AgNPs of comparable sizes and further confirmed the highest antibacterial effect of smaller AgNPs. This is particularly evident in the plot of Fig.2, where the calculated killing trend of *E. coli* after 24h exposure to AgNPs mainly depends on their size, with a higher killing efficiency at lower concentrations by the 6 nm AgNPs followed by 30 nm and 52 nm AgNPs.

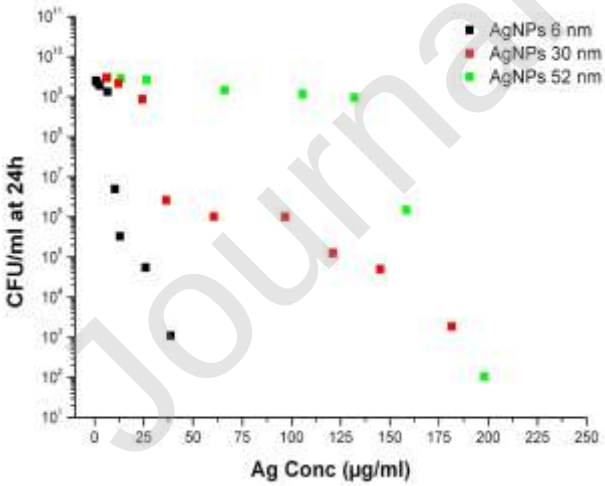

Fig.2: Comparison of the three colloidal AgNPs sizes antibacterial effects with respect to the silver concentration.

Plot of the CFU/ml counted after 24h of incubation of *E. coli* with the colloidal AgNPs 6 nm (black squares), 30 nm (red squares) and 52 nm (green squares) *vs* the silver concentration used for the MIC and MBC experiments.

Table 1: Bactericidal properties characterization of AgNPs colloidal suspensions

AgNPs nominal size (nm)	MIC (µg/ml)	Number of AgNPs at the MIC (NPS/ml)*	Surface Area AgNPs at the MIC (nm^2/ml)*	MBC (µg/ml)	Number of AgNPs at the MBC (NPs/ml)*	Surface Area AgNPs at the MBC (nm^2/ml)*
6	10.4	8.67×10^{12}	9.80×10^{14}	39	3.25×10^{13}	3.68×10^{15}
30	36.4	2.45×10^{11}	6.92×10^{14}	182	1.22×10^{12}	3.46×10^{15}
52	158	1.94×10^{11}	1.7×10^{15}	198	2.42×10^{11}	2.14×10^{15}

* The values were calculated assuming a spherical shape of the AgNPs using the formulas reported in the SI

Moreover, their aggregation state was studied by monitoring the profile of the UV-VIS spectra at different concentrations of AgNPs both in water and in LB broth (Fig. S3 SI). These studies revealed that the aggregation phenomenon is really evident in the culture medium in respect to the water and it increases proportionally with the size and the concentration of the nanoparticles, as indicated by the formation of broad plasmonic bands in the spectral region between 450 nm - 800 nm. This suggests that the killing efficiency associated with the smaller NPs and promoted by their higher specific surface area is probably reduced due to their agglomeration, while bigger AgNPs displayed a comparable bactericidal effect due to their higher silver content. It could be assumed that above a certain concentration value even the smallest AgNPs are no longer capable of penetrating bacterial cells because they are stuck together. Consequently, with the formation of agglomerate that become bigger

with the increase of the AgNPs concentration in liquid, the exposed surface areas become nearly the same for each of the three sizes so the dominant antibacterial effect could be mainly attributed to Ag^+ ions release and direct contact, losing the differences related to the size. Moreover, since the AgNPs are dispersed in a complex medium, the availability of silver ions can be affected by the presence of salts and proteins in the environment which, together with the occurring agglomeration events, could negatively influence their antibacterial efficacy [16,31–33].

Therefore, in order to avoid all this phenomena and better elucidate the bactericidal activity of the AgNPs in respect to their size, they were anchored on a solid surface as monolayers.

3. 3 Preparation and characterization of AgNPs-modified glass substrates

Glass silanization with amino-functional moieties is a well-established method to anchor metallic NPs on the glass surface [18,21]. Different levels of AgNPs surface coverage was obtained by changing NPs concentration and/or the incubation time. UV-VIS analysis together with SEM were first performed to study the attachment of the different types of AgNPs on glass and to evaluate the surface coverage over time.

As example, Fig.3 shows SEM and UV-VIS characterization of four glass substrates incubated for different times with 52 nm AgNPs. As the incubation time increases from 1h to overnight (O/N), the slides color moves from a light yellow to dark yellow, indicating a higher level of surface coverage (Fig.3 a)). This is indeed confirmed by the UV-VIS spectra in Fig.3 b) where a progressive increase of the intensity of the extinction is observed over time. Moreover, as soon as the incubation time is increased, a broad band centered at 600 nm - 800 nm shows up, which is related to the plasmonic coupling of AgNPs in close proximity and to the formation of aggregates on the surface. A similar behavior was also observed in the

samples covered with the 6 nm and 30 nm AgNPs (Fig.S4 SI), where, in addition to the expected and increasing LSPR peaks close to 400 nm, new absorptions around 500 nm (for 6 nm AgNPs) and 650 nm (for 30 nm) appeared and increased with deposition time. SEM analysis (Fig.3 c)) further confirms the progressive surface coverage of AgNPs over time. In particular, at lower incubation times (1 and 2h), all nanoparticles are present in a well-segregated manner with only few nanoclusters of three to six NPs on the surface, thus confirming the single LSPR peak in the extinction spectra at the corresponding times.

The deposition protocols were optimized for each size of AgNPs by changing the incubation time in order to find the optimal conditions to produce a homogeneous and stable monolayer together with a maximized surface coverage, 4 glasses for each size were prepared (Fig.S4-S5 SI). It was observed that for smaller AgNPs a lower incubation time is required to reach the highest surface coverage.

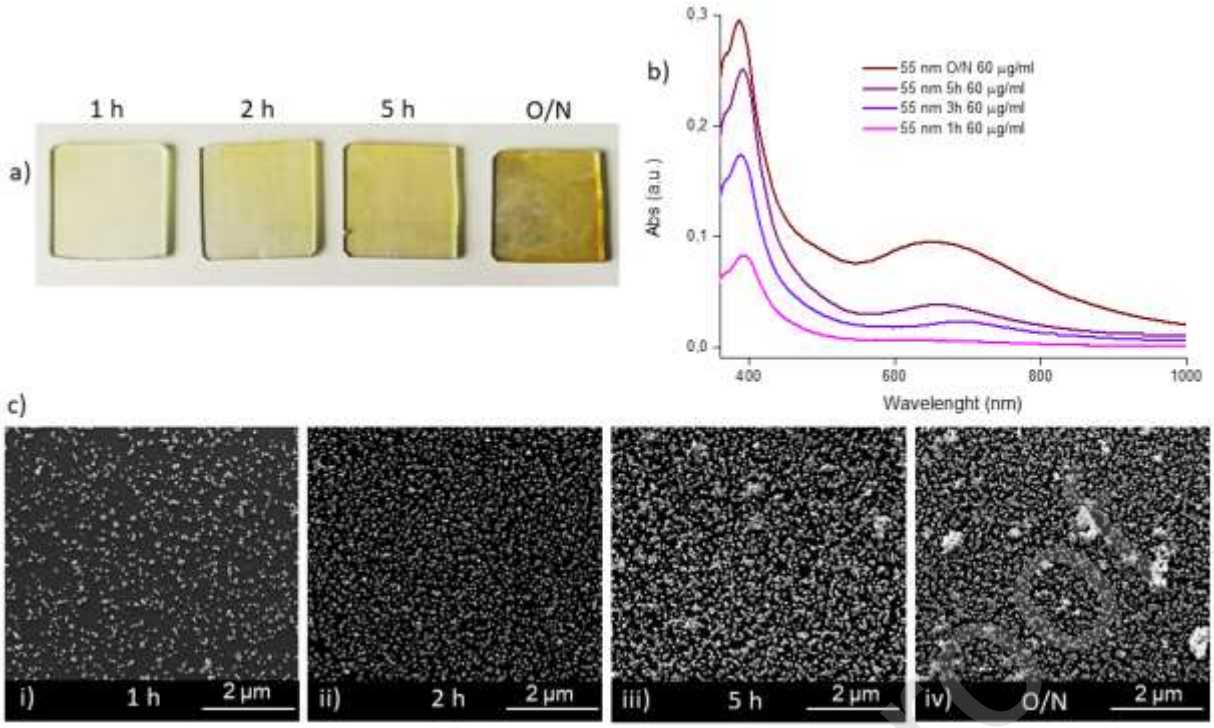

Fig.3 UV-VIS and SEM characterization of AgNPs functionalized glass slides

a) Images of APTES functionalized glass slides incubated with AgNPs 55 nm at a concentration of 59.3 µg/ml for four different time spans (1h, 3h, 5h O/N from left to right respectively) **b)** UV-VIS absorbance spectra of the four AgNPs functionalized glasses described in a **c)** SEM images of the glass slides described in a).

3. 4 Antibacterial characterization of AgNPs functionalized glass substrates

The bactericidal efficacy of glasses obtained with the above mentioned optimized protocols was tested using the ISO 22196:2011 [26] procedure, as widely accepted standard and reliable method for measuring the antibacterial activity of daily goods [34] and to facilitate the comparison of the results between different materials and laboratories. Since some critical physiological factors can influence the outcome of antimicrobial testing, as well descripted in the work of Wiegand et al. [35], all changes to the standard protocol are given in detail in the material and methods section to clarify the experimental procedures and to allow easy reproduction by other laboratories for proper comparisons. All these tested substrates reached

a bacterial killing rate of 99,9999% with almost no bacterial colony present on the agar plates, thus resulting in R values ≥ 5. The R value corresponds to the decimal log reduction rate of viable bacteria, so a surface that reaches an R > 4 is considered an optimum antibacterial material. So, to study the antibacterial effect based on the AgNPs size and to establish the Surface MBC value for each type of active substrate, a wide range of glasses with a different surface coverage were prepared by progressively diluting the concentration of the starting AgNPs suspensions and by testing different deposition times (Fig.4). As Fig.4 shows, the amount of AgNPs deposited on the surfaces was evaluated by UV-VIS characterization (Fig.4 i)), while the antibacterial properties were quantified using the formula:

$R = (U_t - U_0) - (A_t - U_0) = U_t - A_t$.

U_t is the average of the common logarithm of the number of viable bacteria (cells/cm^2), recovered from the untreated test specimens after 5 h; U_0 is the average of the common logarithm of the number of viable bacteria (cells/cm^2), recovered from the untreated test specimens immediately after inoculation; A_t is the average of the common logarithm of the number of viable bacteria (cells/cm^2), recovered from the treated test specimens after 5 h.

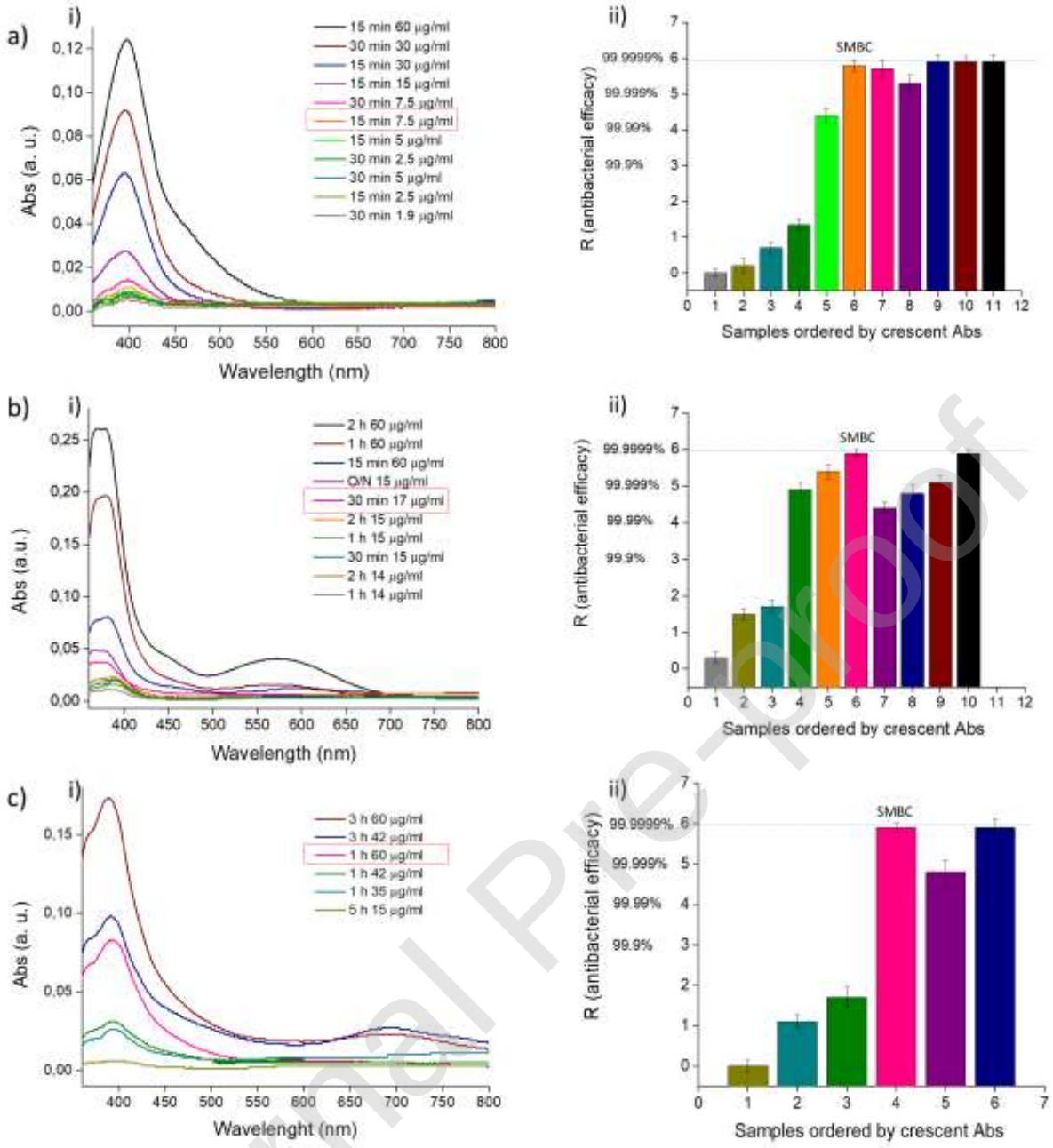

Fig.4 UV-VIS and antibacterial characterization of AgNPs functionalized glass slides

The graphs on the left (i) are the UV-VIS extinction spectra of glass slides functionalized with different concentration of AgNPs incubated for different time spans. The histograms on the right (ii) are the graphical representation of calculated R values of glasses analyzed by UV-VIS ordered by crescent absorbance. a) AgNPS of 6 nm, b) AgNPS of 30 nm and c) AgNPS of 52 nm respectively.

From the graphs reported in Fig.4 it is evident that the antibacterial efficacy is proportional with the AgNPs coverage, with an increasing trend between the extinction intensity of the UV-VIS spectra and the R value. When a certain value of AgNPs coverage is obtained, the R value reaches its maximum around 5.9 and do not rise any further, this represents a bacterial killing $\geq$ 99.9999 %. These samples are indicated as SMBC in Fig 4 ii) and they are the one incubated for 15 min with 7.5 μg/ml of 6 nm AgNPs (R = 5.8), the one incubated for 30 min with 17 μg/ml of 30 nm AgNPs (R = 5.9) and the one incubated for 1 hour with 60 μg/ml of 52 nm AgNPs (R=5.8).

These selected samples were analyzed with ICP-MS to quantify the amount of silver on each surface, which was calculated to be (0.023 ± 0.004) μg/cm^2 for 6 nm AgNPs, (0.026 ± 0.002) μg/cm^2 for 30nm AgNPs and (0.034 ± 0.007) μg/cm^2 for 52 nm AgNPs, respectively. It is interesting to notice how similar AgNPs-modified glasses proposed by Pallavicini *et al.*, [36,37] showed a comparable antibacterial efficacy against *E. coli* ATCC 10356 using an amount of silver at least fifteen times higher than the SMBC reported in this work for 6 nm AgNPs. Thus, the calculation of the SMBC is fundamental to reduce the amount of silver needed to obtain a good antibacterial efficacy, keeping this amount to its minimum.

Moreover, to provide a comparison with the antibacterial tests performed on the colloidal suspensions of AgNPs, the MBC values reported in Table 1 were converted in μg/cm^2 by considering the hypothetical experiment in which 0.1 ml of dispersed AgNPs and 1 x 10^6 CFU/ml of *E. coli* were placed on the top of a non-functionalized glass (see Table S4 in SI). All these results are summarized in Table 2.

Table 2: ICP-MS calculation of anchored AgNPs MBC

AgNPs size (nm)	MBC ($\mu g/cm^2$)*	Number of AgNPs at the MBC in 0.1 ml	Surface Area AgNPs at the MBC (nm^2)	SMBC ($\mu g/cm^2$)	Number of AgNPs at the SMBC	Surface Area AgNPs at the Surface MBC (nm^2)
6 ± 3	0.96	3.25×10^{12}	3.68×10^{15}	0.023	7.73×10^{10}	8.74×10^{12}
30 ± 6	4.5	1.22×10^{11}	3.46×10^{15}	0.026	7.02×10^{8}	1.98×10^{12}
52 ± 7	4.7	2.42×10^{10}	2.14×10^{15}	0.034	1.66×10^{8}	1.47×10^{12}

* The values were calculated using the formulas reported in the SI

A greater bactericidal effect is observed with smaller AgNPs and it progressively decreases with the increasing of the size, which is still in accordance with the antibacterial results obtained with colloidal AgNPs. However, the ratio of the MBC values reported for each type of antibacterial test, i.e. AgNPs in liquid and anchored to the surface, are quite different. In case of the antibacterial test in liquid, the MBC value for the 6 nm AgNPs is almost four and five times lower than the ones reported for 30 nm and 52 nm AgNPs, respectively, while this difference is greatly reduced when the AgNPs are anchored to the surface. In fact, the difference among the SMBC registered on the AgNPs-modified glasses is only statistically significant (p value < 0.05) in respect to the 52 nm AgNPs, while no significant difference was registered between 6 nm and 30 nm AgNPs. This could be due to the reduced penetration ability inside the bacteria by smaller NPs once they are attached to the surface, even if the number of 6 nm AgNPs and their exposed surface area is higher than the 30 nm and 52 nm AgNPs (Table 2).

Moreover, if the MBC of these two sets of experiments are compared, the SMBC are almost two to three orders of magnitude lower than the corresponding values in liquid. These results suggest that the immobilization of the AgNPs on the surface greatly enhances their

bactericidal effects by preventing their aggregation and maximizing their contact with the bacterial cells. This was indeed previously demonstrated by Aghinotri group where citrate capped (8.6 ± 1.2) nm AgNPs displayed higher bactericidal properties when they were anchored on glass in respect to the same size in form of colloidal suspension [18]. Moreover, the antibacterial efficacy of the anchored AgNPs in respect to the colloidal suspensions resulted to be greatly enhanced, probably due to the reduction of the aggregation phenomena, normally occurring in liquid media, which maximizes the exposed specific superficial area of the AgNPs as well as Ag+ ions release and the direct contact with bacterial cells. Furthermore, the differences between the sizes resulted significantly reduced when they are immobilized on a surface, which might be desirably to reduce cytotoxicity related to small NPs [34].

4. Conclusions

Three differently sized spheroidal AgNPs with a diameter of (6, 30 and 52) nm were synthetized, characterized and successfully anchored on amino-silanized glass surfaces. Then, the antibacterial activity against *E. coli* ATCC 8739 was analysed both for colloidal and immobilized AgNPs and, for the first time, a Surface Minimal Bactericidal Concentration (SMBC) was determined for each of the three sizes. In particular, the antibacterial efficacy of a wide range of amino-silanized glasses modified with different concentrations of AgNPs of each size were quantified by the international standard ISO 22196 adapted method. The lowest amount of silver found on AgNPs modified glasses that demonstrated an R∼6 (killing rate ≥ 99.9999 %) for each NPs size was quantified by ICP-MS. These values were considered the SMBC and were respectively 0.023 μg/cm^2, 0.026 μg/cm^2 and 0.034 μg/cm^2

for AgNPs 6 nm, 30 nm and 52 nm. These values demonstrated to be significantly lower in respect to comparable AgNPs modified glass systems, highlighting the importance of the evaluation of the SMBC to minimize the quantity of silver on the surface.

Since this study is based on international standard procedure, which facilitates the comparison of the antibacterial properties of different non-porous surfaces, and allows to define the minimal concentration of a specific biocide to obtain a bacterial killing ≥ 99.9999 %, the calculation of the SMBC could then be extended to a variety of new active materials in many fields to reduce the costs of production and their toxicity to a minimum.

Sample CRediT author statement

Giulia Barzan: Methodology, Investigation, Data Curation, Writing - Original Draft, Writing - Review & Editing. **Luca Rocchetti:** Methodology, Investigation, Data Curation. **Chiara Portesi:** Methodology, Data Curation. **Francesco Pellegrino:** Methodology, Investigation, Data Curation. **Angelo Taglietti**: Conceptualization, Writing - Review & Editing. **Andrea M. Rossi:** Funding acquisition, Supervision, Writing - Review & Editing. **Andrea M. Giovannozzi:** Conceptualization, Resources, Data Curation, Writing - Review & Editing, Supervision.

Declaration of interests

The authors declare that they have no known competing financial interests or personal relationships that could have appeared to influence the work reported in this paper.

Acknowledgements

We thank Lavinia Rita Doveri (University of Pavia) for her precious advice. We would like to pay our gratitude and respects to our colleague Prof. Gianmario Martra who recently passed away. He was a dedicated professor in the Department of Chemistry and NIS Inter-Departmental Centre at the University of Torino, with a passion for research pertaining to the investigation of the physic-chemical and chemical events resulting from the adsorption of molecules on surfaces of nanomaterials, and an exceptional mentor for most of us, always encouraging and supporting young scientists career. He was honored with numerous awards and recognitions for both his teaching and his research. He certainly was in our thoughts in putting together this scientific contribution. This research did not receive any specific grant from funding agencies in the public, commercial, or not-for-profit sectors.

References

[1] J.S. Kim, E. Kuk, K.N. Yu, J.H. Kim, S.J. Park, H.J. Lee, S.H. Kim, Y.K. Park, Y.H. Park, C.Y. Hwang, Y.K. Kim, Y.S. Lee, D.H. Jeong, M.H. Cho, Antimicrobial effects of silver nanoparticles, Nanomedicine Nanotechnology, Biol. Med. 3 (2007) 95–101. https://doi.org/10.1016/j.nano.2006.12.001.

[2] Z. Huang, X. Jiang, D. Guo, N. Gu, Controllable synthesis and biomedical applications of silver nanomaterials, J. Nanosci. Nanotechnol. 11 (2011) 9395–9408. https://doi.org/10.1166/jnn.2011.5317.

[3] G. P., G. C., S. X., Z. Q., L. S.S., T. C., C. Y., C.-P. M.B., C. M.W., W. K., X. R., P. Gunawan, C. Guan, X. Song, Q. Zhang, S.S. Leong, C. Tang, Y. Chen, M.B. Chan-Park, M.W. Chang, K. Wang, R. Xu, Hollow fiber membrane decorated with Ag/MWNTs: toward effective water disinfection and biofouling control, ACS Nano. 5 (2011) 10033–10040. https://doi.org/10.1021/nn2038725; 10.1021/nn2038725.

[4] W.R. Li, X.B. Xie, Q.S. Shi, H.Y. Zeng, Y.S. Ou-Yang, Y. Ben Chen, Antibacterial activity and mechanism of silver nanoparticles on Escherichia coli, Appl. Microbiol. Biotechnol. 85 (2010) 1115–1122. https://doi.org/10.1007/s00253-009-2159-5.

[5] S. Chernousova, M. Epple, Silver as antibacterial agent: Ion, nanoparticle, and metal, Angew. Chemie - Int. Ed. 52 (2013) 1636–1653. https://doi.org/10.1002/anie.201205923.

[6] P.L. Drake, K.J. Hazelwood, Exposure-related health effects of silver and silver

compounds: A review, Ann. Occup. Hyg. (2005). https://doi.org/10.1093/annhyg/mei019.

[7] M. Carbone, D.T. Donia, G. Sabbatella, R. Antiochia, Silver nanoparticles in polymeric matrices for fresh food packaging, J. King Saud Univ. - Sci. (2016). https://doi.org/10.1016/j.jksus.2016.05.004.

[8] M.L.W. Knetsch, L.H. Koole, New strategies in the development of antimicrobial coatings: The example of increasing usage of silver and silver nanoparticles, Polymers (Basel). (2011). https://doi.org/10.3390/polym3010340.

[9] D. Gangadharan, K. Harshvardan, G. Gnanasekar, D. Dixit, K.M. Popat, P.S. Anand, Polymeric microspheres containing silver nanoparticles as a bactericidal agent for water disinfection, Water Res. (2010). https://doi.org/10.1016/j.watres.2010.06.057.

[10] C.N. Baker, S.A. Stocker, D.H. Culver, C. Thornsberry, Comparison of the E test to agar dilution, broth microdilution, and agar diffusion susceptibility testing techniques by using a special challenge set of bacteria, J. Clin. Microbiol. 29 (1991) 533–538.

[11] J.R. Morones, J.L. Elechiguerra, A. Camacho, K. Holt, J.B. Kouri, J.T. Ramírez, M.J. Yacaman, The bactericidal effect of silver nanoparticles, Nanotechnology. 16 (2005) 2346–2353. https://doi.org/10.1088/0957-4484/16/10/059.

[12] S. Agnihotri, S. Mukherji, S. Mukherji, Size-controlled silver nanoparticles synthesized over the range 5-100 nm using the same protocol and their antibacterial efficacy, RSC Adv. 4 (2014) 3974–3983. https://doi.org/10.1039/c3ra44507k.

[13] E. Amato, Y.A. Diaz-Fernandez, A. Taglietti, P. Pallavicini, L. Pasotti, L. Cucca, C. Milanese, P. Grisoli, C. Dacarro, J.M. Fernandez-Hechavarria, V. Necchi, Synthesis, characterization and antibacterial activity against gram positive and gram negative bacteria of biomimetically coated silver nanoparticles, Langmuir. 27 (2011) 9165–9173. https://doi.org/10.1021/la201200r.

[14] G.A. Sotiriou, S.E. Pratsinis, Engineering nanosilver as an antibacterial, biosensor and bioimaging material, Curr. Opin. Chem. Eng. 1 (2011) 3–10. https://doi.org/10.1016/j.coche.2011.07.001.

[15] S. Pal, Y.K. Tak, J.M. Song, Does the antibacterial activity of silver nanoparticles depend on the shape of the nanoparticle? A study of the gram-negative bacterium Escherichia coli, Appl. Environ. Microbiol. 73 (2007) 1712–1720. https://doi.org/10.1128/AEM.02218-06.

[16] L. Kvítek, A. Panáček, J. Soukupová, M. Kolář, R. Večeřová, R. Prucek, M. Holecová, R. Zbořil, Effect of surfactants and polymers on stability and antibacterial activity of silver nanoparticles (NPs), J. Phys. Chem. C. 112 (2008) 5825–5834. https://doi.org/10.1021/jp711616v.

[17] A.K. Ostermeyer, C. Kostigen Mumuper, L. Semprini, T. Radniecki, Influence of bovine serum albumin and alginate on silver nanoparticle dissolution and toxicity to Nitrosomonas europaea, Environ. Sci. Technol. (2013). https://doi.org/10.1021/es4033106.

[18] S. Agnihotri, S. Mukherji, S. Mukherji, Immobilized silver nanoparticles enhance

contact killing and show highest efficacy: Elucidation of the mechanism of bactericidal action of silver, Nanoscale. (2013). https://doi.org/10.1039/c3nr00024a.

[19] F. Furno, K.S. Morley, B. Wong, B.L. Sharp, P.L. Arnold, S.M. Howdle, R. Bayston, P.D. Brown, P.D. Winship, H.J. Reid, Silver nanoparticles and polymeric medical devices: A new approach to prevention of infection?, J. Antimicrob. Chemother. (2004). https://doi.org/10.1093/jac/dkh478.

[20] N. Durán, P.D. Marcato, G.I.H. De Souza, O.L. Alves, E. Esposito, Antibacterial effect of silver nanoparticles produced by fungal process on textile fabrics and their effluent treatment, J. Biomed. Nanotechnol. (2007). https://doi.org/10.1166/jbn.2007.022.

[21] A. Taglietti, C.R. Arciola, A. D'Agostino, G. Dacarro, L. Montanaro, D. Campoccia, L. Cucca, M. Vercellino, A. Poggi, P. Pallavicini, L. Visai, Antibiofilm activity of a monolayer of silver nanoparticles anchored to an amino-silanized glass surface, Biomaterials. (2014). https://doi.org/10.1016/j.biomaterials.2013.11.047.

[22] Y. Wan, Z. Guo, X. Jiang, K. Fang, X. Lu, Y. Zhang, N. Gu, Quasi-spherical silver nanoparticles: Aqueous synthesis and size control by the seed-mediated Lee-Meisel method, J. Colloid Interface Sci. 394 (2013) 263–268. https://doi.org/10.1016/j.jcis.2012.12.037.

[23] L. Mandrile, I. Cagnasso, L. Berta, A.M. Giovannozzi, M. Petrozziello, F. Pellegrino, A. Asproudi, F. Durbiano, A.M. Rossi, Direct quantification of sulfur dioxide in wine by Surface Enhanced Raman Spectroscopy, Food Chem. (2020). https://doi.org/10.1016/j.foodchem.2020.127009.

[24] L. Mandrile, M. Vona, A.M. Giovannozzi, J. Salafranca, G. Martra, A.M. Rossi, Migration study of organotin compounds from food packaging by surface-enhanced Raman scattering, Talanta. (2020). https://doi.org/10.1016/j.talanta.2020.121408.

[25] M.D. Abràmoff, P.J. Magalhães, S.J. Ram, Image processing with imageJ, Biophotonics Int. (2004). https://doi.org/10.1201/9781420005615.ax4.

[26] I. 61851, International Standard International Standard, 61010-1 © Iec2001. 2006 (2006) 13.

[27] F. Quan, A. Mao, M. Ding, S. Ran, J. Wang, G. Yang, Y. Yan, Combustion synthesis and formation mechanism of silver nanoparticles, Int. J. Mater. Res. 109 (2018) 751–755. https://doi.org/10.3139/146.111666.

[28] M. Chen, Y.G. Feng, X. Wang, T.C. Li, J.Y. Zhang, D.J. Qian, Silver nanoparticles capped by oleylamine: Formation, growth, and self-organization, Langmuir. (2007). https://doi.org/10.1021/la700553d.

[29] R.X. He, R. Liang, P. Peng, Y. Norman Zhou, Effect of the size of silver nanoparticles on SERS signal enhancement, J. Nanoparticle Res. (2017). https://doi.org/10.1007/s11051-017-3953-0.

[30] 2007, Performance Standards for Antimicrobial Susceptibility Testing, 2007. https://doi.org/1-56238-525-5.

[31] S. Tang, J. Zheng, Antibacterial Activity of Silver Nanoparticles: Structural Effects, Adv. Healthc. Mater. (2018). https://doi.org/10.1002/adhm.201701503.

[32] Y.M. Long, L.G. Hu, X.T. Yan, X.C. Zhao, Q.F. Zhou, Y. Cai, G. Bin Jiang, Surface ligand controls silver ion release of nanosilver and its antibacterial activity against Escherichia coli, Int. J. Nanomedicine. (2017). https://doi.org/10.2147/IJN.S132327.

[33] T.S. Radniecki, D.P. Stankus, A. Neigh, J.A. Nason, L. Semprini, Influence of liberated silver from silver nanoparticles on nitrification inhibition of Nitrosomonas europaea, Chemosphere. (2011). https://doi.org/10.1016/j.chemosphere.2011.06.039.

[34] Y. Ando, H. Miyamoto, I. Noda, F. Miyaji, T. Shimazaki, Y. Yonekura, M. Miyazaki, M. Mawatari, T. Hotokebuchi, Effect of bacterial media on the evaluation of the antibacterial activity of a biomaterial containing inorganic antibacterial reagents or antibiotics, Biocontrol Sci. (2010). https://doi.org/10.4265/bio.15.15.

[35] C. Wiegand, A. Völpel, A. Ewald, M. Remesch, J. Kuever, J. Bauer, S. Griesheim, C. Hauser, J. Thielmann, S. Tonndorf-Martini, B.W. Sigusch, J. Weisser, R. Wyrwa, P. Elsner, U.C. Hipler, M. Roth, C. Dewald, C. Lüdecke-Beyer, J. Bossert, Critical physiological factors influencing the outcome of antimicrobial testing according to ISO 22196 / JIS Z 2801, PLoS One. (2018). https://doi.org/10.1371/journal.pone.0194339.

[36] P. Pallavicini, A. Taglietti, G. Dacarro, Y. Antonio Diaz-Fernandez, M. Galli, P. Grisoli, M. Patrini, G. Santucci De Magistris, R. Zanoni, Self-assembled monolayers of silver nanoparticles firmly grafted on glass surfaces: Low Ag+ release for an efficient antibacterial activity, J. Colloid Interface Sci. 350 (2010) 110–116. https://doi.org/10.1016/j.jcis.2010.06.019.

[37] G. Dacarro, L. Cucca, P. Grisoli, P. Pallavicini, M. Patrini, A. Taglietti, Monolayers of

polyethilenimine on flat glass: A versatile platform for cations coordination and nanoparticles grafting in the preparation of antibacterial surfaces, Dalt. Trans. (2012). https://doi.org/10.1039/c1dt11373a.